VIBRATIONAL SPECTRA AND FRONTIER MOLECULAR ORBITAL ANALYSIS OF 2-(4-METHOXYPHENYL)-4, 5-DIPHENYL-1H-IMIDAZOLE

S. Jeya[1], B. Revathi[1,*], V. Balachandran[1], B. Narayana[2]
[1]Centre for Research-Department of Physics, A. A.Government Arts College, Musiri, Tiruchirappalli 621 211, India.
[2]Department of Studies in Chemistry, Mangalore University, Mangalagangotri 574 199, India.

Abstract:

The FT-IR and FT-Raman spectra of 2-(4-Methoxyphenyl)-4, 5-diphenyl-1H-imidazole (MPDPI) molecule have been recorded in the region 4000-400 cm^{-1} and 3500-100 cm^{-1} respectively. Optimized geometrical structure, harmonic vibrational frequencies, and intensities have been computed by the B3LYP density functional levels using ccpVDZ and 6-311G basis sets. The observed FT-IR and FT-Raman vibrational frequencies are analyzed. The geometries and normal modes of vibration obtained from DFT method are in good agreement with the experimental data. The charge transfer occurring in the molecule between HOMO and LUMO energies, frontier energy gap, the molecular electrostatic potential (MEP) were calculated and analyzed.

Keywords: 2-(4-Methoxyphenyl)-4, 5-diphenyl-1H-imidazole; Vibrational spectra; MEP Surface.

1. INTRODUCTION

Imidazole is incorporated into many important biological molecules. The most pervasive is the amino acid histidine, which has an Imidazole side-chain. Histidine is present in many proteins and enzymes and plays a vital part in the structure and binding functions of hemoglobin. Imidazole-based histidine compounds play a very important role in intracellular buffering[1]. Histidine can be decarboxylated to histamine, which is also a common biological compound. It can cause urticaria (hives) when histamine is produced during the allergic reaction.

Imidazole has become an important part of many pharmaceuticals. Synthetic imidazoles are present in many fungicides and antifungal, antiprotozoal, and antihypertensive medications. Imidazole is part of the theophylline molecule, found in tea leaves and coffee beans, that stimulate the central nervous system. It is present in the anticancer medication mercaptopurine, which combats leukemia by interfering with DNA activities.

A number of substituted imidazoles, including clotrimazole, are selective inhibitors of nitric oxide synthase, which makes them interesting drug targets in inflammation, neurodegenerative diseases and tumors of the nervous system[2-3]. Other biological activities of the imidazole pharmacophore relate to the downregulation of intracellular Ca++ and K+ fluxes, and interference with translation initiation[4].

The substituted imidazole derivatives are valuable in the treatment of many systemic fungal infections[5]. Imidazoles belong to the class of azole antifungals, which includes ketoconazole, miconazole, and clotrimazole.

Some attempts were made for the interpretations of the vibrational spectra of imidazole derivatives[6]. Literature survey reveals that to the best of our knowledge, the results based on quantum chemical calculations, FT-IR and FT-Raman spectral analyses of 2-(4-Methoxyphenyl)-4, 5-diphenyl-1H-imidazole (MPDPI) have no reports.

In the present work, an attempt have been made to interpret the vibrational spectra of MPDPI by using B3LYP level of theory throughout with the ccpVDZ and 6-311G basis sets are implemented in the Gaussian 09 program suite[7]. A detailed interpretations of the infrared and Raman spectra based on the theoretical results, which are acceptable and supportable to each other.

2. EXPERIMENTAL DETAILS

The room temperature Fourier Transform infrared spectrum of MPDPI was measured in the 4000-400cm^{-1} region at a resolution of ± 1cm^{-1} using BRUKER IFS-66V FT-IR Spectrometer equipped with a KBr pellet were used in the spectral measurements. The FT-Raman spectrum was recorded on a BRUKER IFS-66V model interferometer equipped with an FRA -106 FT-Raman accessories in the 3500-100 cm^{-1} stokes region using the 1064nm line of an Nd: YAG laser for excitation operating at 200mW power.

3. COMPUTATIONAL DETAILS

The molecular structure of MPDPI and corresponding vibrational harmonic frequencies were calculated Gaussian 09 software package[7] at the DFT (B3LYP) levels supplemented with the standard ccpVDZ and 6-311G basis sets, without any constraint on the geometry. The harmonic vibrational frequencies have been analytically calculated by taking the second-order derivative of energy using the same level of theory. Transformation of force field from Cartesian to symmetry coordinate, scaling, subsequent normal coordinate analysis, and calculations of TED were made with the version V7.0-G77 of the MOLVIB program written by Sundius[8,9]. To achieve a close agreement between observed and calculated frequencies, the least-square fit refinement algorithm was used. By combining the results of the GAUSSVIEW[10] program with symmetry considerations, along with the available related molecules, vibrational frequency assignments were made with a fairly high degree of accuracy. For the plots of simulated IR and Raman spectra, pure Lorentzian band shapes were used with a bandwidth of ±1 cm^{-1}. Prediction of Raman intensities was carried out by the following procedure. The Raman activities (Si) calculated by the Gaussian 09 program were converted to relative Raman intensities (Ii) using the following relationship derived from the basic theory of scattering.

$$I_i = \frac{f(\nu_0 - \nu_i)^4 s_i}{\nu_i[1-\exp(\frac{-hc\nu_i}{kt})]} \quad \ldots\ldots\ldots\ldots\ldots (1)$$

where ν_0 is the exciting wavenumber (cm^{-1} units ν_i is the vibrational wavenumber of the i^{th} normal mode, h, c, and k are universal constant and f is a suitably chosen common normalization factor for all peak intensities.

4. RESULT AND DISCUSSION

Molecular geometry

The molecular structure of MPDPI along with numbering of atoms is shown in Fig. 1. The maximum number of potentially active observable fundamentals of a non-liner molecule that contains N atoms is equal to (3n-6), apart from three translational and three rotational degrees of freedom [11]. BI having 43 atoms with 123 Normal modes of vibrations which are distributed amongst the symmetry species as $(3N-6)_{vib}$=83A' (in-plane) + 40A" (out-of-plane). The A' vibrations are totally symmetric and give rise to polarized Raman lines whereas A" vibrations are antisymmetric and give rise to depolarized Raman lines. The observed and simulated spectra of the title compound are shown in Figs. 2 and 3 respectively. The most optimized geometrical parameters (bond length, bond angle) were also calculated by B3LYP/6-31G and B3LYP/6-311+G basis sets, which are depicted in Table 1.

Fig.1. Optimized geometrical structure and atomic labeling of 2-(4-Methoxyphenyl)-4,5-diphenyl-1H-imidazole

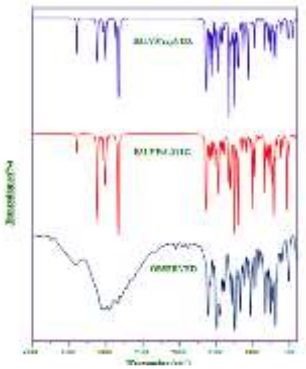

Fig.2 Observed and simulated FT-IR spectra of 2-(4-Methoxyphenyl)-4,5-diphenyl-1H-imidazole

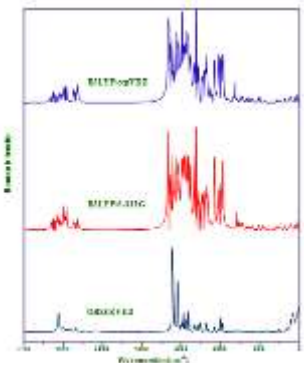

Fig.3 Observed and simulated FT-Raman spectra of 2-(4-Methoxyphenyl)-4,5-diphenyl-1H-imidazole

Table 1 Optimized geometrical parameters of MPDPI by B3LYP/ccpVdZ and B3LYP/6-311(G)

	Bond length			Bond angle	
Parameters	B3LYP/ ccpVDZ	B3LYP/6-311G	Parameters	B3LYP/ ccpVDZ	B3LYP/6-311G
C1-C2	1.40	1.40	C2-C1-C6	118.76	118.74
C1-C6	1.40	1.40	C2-C1-C12	120.60	120.62
C1-C12	1.49	1.48	C6-C1-C12	120.60	120.62
C2-C3	1.40	1.40	C1-C2-C3	120.64	120.65
C2-H7	1.09	1.08	C1-C2-H7	119.20	119.19

C3-C4	1.40	1.40	C3-C2-H7	120.16	120.16
C3-H8	1.09	1.08	C2-C3-C4	120.14	120.13
C4-C5	1.40	1.40	C2-C3-H8	119.78	119.79
C4-H9	1.09	1.08	C4-C3-H8	120.08	120.08
C5-C6	1.40	1.40	C3-C4-C5	119.68	119.69
C5-H10	1.09	1.08	C3-C4-H9	120.16	120.15
C6-H11	1.09	1.08	C5-C4-H9	120.16	120.15
C12-C13	1.40	1.40	C4-C5-C6	120.14	120.13
C12-N16	1.37	1.39	C4-C5-H10	120.08	120.08
C13-N14	1.39	1.40	C6-C5-H10	119.78	119.79
C13-C18	1.47	1.46	C1-C6-C5	120.64	120.65
N14-C15	1.37	1.38	C1-C6-H11	119.20	119.19
N14-H17	1.01	1.00	C5-C6-H11	120.16	120.16
C15-N16	1.33	1.34	C1-C12-C13	129.76	130.22
C15-C29	1.46	1.46	C1-C12-N16	119.64	119.58
C18-C19	1.41	1.41	C13-C12-N16	110.60	110.20
C18-C20	1.41	1.41	C12-C13-N14	103.75	104.21
C19-C21	1.40	1.39	C12-C13-C18	134.17	133.79
C19-H22	1.09	1.08	N14-C13-C18	122.08	122.00
C20-C23	1.39	1.39	C13-N14-C15	108.88	109.07
C20-H24	1.09	1.08	C13-N14-H17	125.36	125.14
C21-C25	1.40	1.40	C15-N14-H17	125.76	125.79
C21-H26	1.09	1.08	N14-C15-C16	110.33	109.60
C23-C25	1.40	1.40	N14-C15-C29	124.66	125.28
C23-H27	1.09	1.08	N16-C15-C29	125.01	125.12
C25-H28	1.09	1.08	C12-C16-C15	106.45	106.92
C29-C30	1.40	1.40	C13-C18-C19	121.20	121.25
C29-C31	1.41	1.41	C13-C18-C20	121.43	121.31
C30-C32	1.40	1.40	C19-C18-C20	117.37	117.44
C30-H33	1.09	1.08	C18-C19-C21	121.43	121.37
C31-C34	1.39	1.39	C18-C19-H22	120.70	120.70
C31-H35	1.09	1.08	C21-C19-H22	117.87	117.93
C32-C36	1.40	1.40	C18-C20-C23	121.03	121.00
C32-H37	1.09	1.08	C18-C20-H24	119.67	119.72
C34-C36	1.41	1.40	C23-C20-H24	119.30	119.28
C34-H38	1.09	1.08	C19-C21-C25	120.39	120.37
C36-O39	1.36	1.39	C19-C21-H26	119.40	119.48
O39-C40	1.42	1.45	C25-C21-H26	120.20	120.15
C40-H41	1.10	1.09	C20-C23-C25	120.82	120.74
C40-H42	1.10	1.09	C20-C23-H27	119.16	119.24
C40-H43	1.10	1.08	C25-C23-H27	120.02	120.02

Vibrational Assignments

The detailed vibrational analysis of fundamental modes of MPDPI along with the FT-IR and FT-Raman experimental frequencies and the unscaled and scaled vibrational frequencies using B3LYP/ ccpVDZ and 6-31+G basis sets are presented in Table 2.

N-H Vibrations

The compounds containing an N-H group exhibit N-H stretching absorption in the region from 3500 to 3200cm^{-1}. The position of absorption depends upon the degree of hydrogen bonding and hence upon the physical state of the sample [12]. The nitrogen and hydrogen bonds present in the title compound will give rise to N-H stretching, in-plane, and out-of-plane bending vibrations. In this study, the FT-IR band appearing at 3410cm^{-1} was designated to N-H stretching vibrations. The bands at 1291cm^{-1} and 1290cm^{-1} are appeared to in-plane bending modes of N-H.

C–H vibrations

Aromatic compounds commonly exhibit multiple weak bands in the region 3100–3000cm^{-1} due to aromatic C–H stretching vibrations[13–15]. The bands appeared at 3056, 3027, 2997, 2960, 2837cm^{-1} in the FT-IR spectrum and 2839cm^{-1} in FT-Raman spectrum are assigned to C–H ring stretching vibrations. The band identified at 3060, 3030, 3025, 3122, 3120, 3117, 3112, 3008, 3001, 2993, 2967, 2957, 2864, 2841cm^{-1} in B3LYP/6-311G methods are assigned to C–H ring stretching vibrations. The C–H in-plane and out-of-plane bending vibrations generally lie in the range 1000–1300cm^{-1} and 950–800cm^{-1}[16], respectively. In the present case, fourteen C–H in-plane bending vibrations of the title compound identified at 1301, 1206, 1200, 1180, 1171, 1162, 1128, 1112, 1085, 1082, 975, 971, 910 and 901cm^{-1} in the B3LYP/6-311G method are assigned to C–H in-plane bending vibrations. The C–H out-of-plane bending vibrations are observed at 830, 696, 513cm^{-1} in FT-IR spectrum and 695, 537, 524, 405, 351, 300 cm^{-1} in FT-Raman spectrum. According to the literature, the in-plane and out-of-plane bending vibrations are found to be lower than their characteristic regions due to the substitution of the OCH_3.

CH_3 vibrations

For the assignments of CH_3 group frequencies, one can expect nine fundamentals. In imidazole group has 9 vibrational modes (2 asymmetrical stretching, 1 symmetrical stretching, in-plane bending, 1 out-of-plane bending, 1 symmetric bending, 1 in-plane rocking, 1 out-of-plane rocking and 1 twisting mode). The CH methyl group stretching vibrations are generally observed in the region 3000–2800 cm^{-1}[17, 18]. Accordingly, in the present the study, the calculated values by B3LYP/ccpVDZ method at 2835, 2830 and 2822 cm^{-1} for CH_3 asymmetric and symmetric stretching vibrations of the methyl group in MPDPI. The CH_3 in-plane bending vibrations have been assigned at 1473 and 1444 cm^{-1} in FT-Raman, C-H out-of-plane bending vibrations calculated at 1193 and 1158 cm^{-1} in B3LYP/ ccpVDZ method. . These assignments are validated by the reported literature [19, 20].

CC vibrations

The ring C-C stretching vibrations, known as semicircle stretching usually occurs in the region 1400-1625cm^{-1}[21-24]. The C-C stretching vibrations of the present compound are observed at 1611, 1580, 1544, 1493, 1249cm^{-1} in the FT-IR spectrum and 1611, 1573, 1545, 1493, 1326, 1209cm^{-1} in FT-Raman spectrum. All the bands lie in the expected range when compared to the literature values. In our present study, the bands for C-C in-plane bending vibrations are observed at 837, 739cm^{-1} and 841cm^{-1} respectively, in FT-IR and FT-Raman spectra. The CCC in-plane bending vibrations observed at 837, 740, 719, cm^{-1}. These assignments are in good agreement with the literature [25, 26]. These observed frequencies show that the substitutions in the ring to some extent to affect the ring modes of vibrations. The theoretically computed value by B3LYP/6-311G methods are in agreement with experimental values.

Table 2 Vibrational assignments of fundamental observed frequencies and calculated frequencies of MPDPI by B3LYP/ccpVDZ B3LYP/6-311G.

Moed No.	Symmetry species	Observed frequencies		Calculated frequencies				Vibrational assignments / %
				Unscaled		Scaled		
		FT-IR	FT-Raman	B3LYP/ ccpVDZ	B3LYP/ 6-311G	B3LYP/ ccpVDZ	B3LYP/ 6-311G	
1	A’	3410		3654	3685	3396	3398	υNH(99)
2	A’	3056	3059	3230	3224	3058	3060	υCH(98)
3	A’	3027		3219	3216	3034	3030	υCH(98)
4	A’			3218	3206	3030	3025	υCH(97)
5	A’			3200	3199	3127	3122	υCH(98)
6	A’			3200	3196	3123	3120	υCH(97)
7	A’			3198	3196	3119	3117	υCH(98)
8	A’			3194	3187	3114	3112	υCH(98)
9	A’			3187	3179	3009	3008	υCH(94)
10	A’			3185	3178	3003	3001	υCH(95)
11	A’	2997		3177	3168	2995	2993	υCH(96)
12	A’			3176	3167	2972	2967	υCH(92)
13	A’	2960		3168	3159	2958	2957	υCH(90)
14	A’			3164	3155	2867	286	υCH(93)
15	A’	2837	2839	3163	3154	2840	2841	υCH(98)
16	A’			3139	3151	2835	2837	υCH_{3asym}(90)
17	A’			3066	3072	2830	2831	υCH_{3asym}(91)
18	A’			3000	3004	2822	2825	υCH_{3sym}(90)
19	A’			1668	1656	1640	1641	υCC(69), δCH(24)
20	A’			1660	1652	1635	1635	υCC(70), δCH(22)
21	A’			1655	1645	1630	1627	υCC(61), δCH(20)
22	A’			1628	1621	1621	1618	υCC(58), δCH(27)
23	A’	1611	1611	1626	1616	1610	1612	υCC(66), δCH(26)
24	A’			1625	1614	1595	1597	υCC(59), δCH(29)
25	A’	1580		1597	1593	1584	1583	υCC(52), δCN(27), δNH(16)
26	A’		1573	1574	1578	1570	1575	υCC(69), δCN(24)
27	A’	1544	1545	1541	1555	1546	1544	υCC(52), δCH(30)
28	A’			1521	1539	1520	1521	υCN(55), δCO(17), δCH(14)

29	A’	1493	1493	1502	1533	1496	1495	υCC(65), δCH(22)
30	A’			1482	1526	1477	1471	υCN(66), δCO(24),
31	A’		1473	1474	1517	1468	1466	$\delta CH_{3\ sb}$(67)
32	A’			1470	1492	1460	1461	υCC, (55), δCH(29)
33	A’			1468	1490	1457	1456	υCC, (66), δCH(21)
34	A’			1461	1489	1453	1451	$\delta CH_{3\ ipb}$ (64)
35	A’	1446	1444	1457	1468	1447	1445	$\delta CH_{3\ ipr}$ (61)
36	A’	1408	1409	1433	1430	1410	1412	υCN(62), δNH(15)
37	A’	1386		1420	1396	1385	1386	υCN(66) , δNH(31)
38	A’		1326	1363	1390	1325	1327	υCC(63), δCH(25)
39	A’			1355	1378	1322	1324	υCC, (55), δCH(28)
40	A’			1349	1358	1319	1319	υCC, (58), δCH(17)
41	A’			1335	1337	1315	1313	υCC, (66), δCN(17), δCH(15)
42	A’			1318	1329	1311	1309	υCC(56), δCH(16), δNH(14)
43	A’			1313	1317	1303	1301	δCH(65), δCN(24)
44	A’	1291	1290	1302	1314	1293	1295	δNH(66), δCN(18)
45	A’		1260	1290	1266	1260	1262	υCO(59), δCC(28),
46	A’	1249		1273	1263	1245	1246	υCC(57)
47	A’		1209	1229	1242	1210	1208	υCC(65), δCN(18)
48	A’	1200		1209	1224	1203	1206	δCH(66), δCO(31)
49	A’			1196	1219	1200	1200	δCH(63), δCH(30)
50	A’’			1190	1215	1194	1193	$\gamma CH_{3\ opb}$(52)
51	A’	1177	1179	1189	1211	1175	1180	δCH(58), CH_{2twist}(32)
52	A’			1173	1211	1170	1171	δCH(58), υCC(25)
53	A’			1170	1199	1164	1162	δCH(58)
54	A’’		1158	1158	1159	1158	1158	$\gamma CH_{3\ opr}$(59)
55	A’	1129		1133	1151	1130	1128	δCH(44)
56	A’		1110	1121	1131	1116	1112	δCH(50)
57	A’		1085	1105	1114	1086	1085	δCH(53)
58	A’		1079	1095	1107	1080	1082	δCH(57)
59	A’	1070		1094	1097	1071	1072	υCC(58), δCH(29)
60	A’		1061	1071	1060	1063	1060	υCO (57)
61	A’	1030		1056	1055	1033	1036	υCC (49)
62	A’		1024	1048	1039	1022	1024	υCC (48)
63	A’			1020	1035	1019	1017	$\delta Ring4_{trigd}$(65)
64	A’			1016	1029	1010	1009	$\delta Ring2_{trigd}$(59)
65	A’			1010	1029	1004	1003	$\delta Ring3_{trigd}$(61)
66	A’			1009	1023	1000	1001	$\delta Ring2_{asy}$(65)
67	A’			1008	1020	999	998	$\delta Ring3_{asy}$(68)
68	A’		998	1008	1018	995	994	$\delta Ring4_{asy}$(67)
69	A’		976	989	1005	980	980	δCN (60), δCH(23)
70	A’			988	998	976	975	δCH(61)
71	A’	969		980	996	971	971	δCH(53)
72	A’			974	982	965	966	δCN(53), δNH(19)
73	A’	913		939	958	911	910	δCH(43)
74	A’		902	932	947	904	901	δCH(54)
75	A’		890	920	939	887	886	δCO(58)
76	A’		841	870	880	837	837	δCC(53), δCH(17)
77	A’’			863	877	835	835	γCH(60)
78	A’’	830		842	860	830	831	γCH(60)

79	A’			816	831	810	808	δCO(43)
80	A’	797		815	810	792	790	$\delta Ring4_{sym}$(65)
81	A’		791	793	807	788	786	$\delta Ring3_{sym}$(59)
82	A’	766	768	790	803	762	761	$\delta Ring2_{sym}$(54)
83	A’	739		759	764	740	740	δCC(44)
84	A’		730	745	751	732	731	δCN(53)
85	A’			723	733	720	719	δCC(43)
86	A’	715		715	728	715	715	δRing1(47)
87	A’		705	711	717	710	709	δCN(53)
88	A’’	696	695	703	714	693	693	γCH(43)
89	A’’		671	685	703	670	668	$\gamma Ring2_{trigd}$(46)
90	A’’	637	635	649	666	632	630	$\gamma Ring4_{trigd}$(65)
91	A’’			632	653	626	625	$\gamma Ring3_{trigd}$(51)
92	A’’		622	630	650	621	620	$\gamma Ring2_{asy}$(45)
93	A’’	613		627	630	610	610	$\gamma Ring4_{asy}$(55)
94	A’		598	608	617	595	594	δRing1(43)
95	A’’		537	553	593	533	531	γCH(50)
96	A’’		524	533	560	520	519	γCH(58)
97	A’’	513		521	527	510	512	γCH(54)
98	A’’			475	525	501	500	γCH(52)
99	A’’			462	475	463	463	γNH(57)
100	A’’			444	451	440	439	γCH(58)
101	A’’			436	440	431	430	γCN(60), δNH(19)
102	A’’			418	428	420	420	$\gamma Ring3_{asy}$(55)
103	A’’		405	413	422	400	398	γCH(46)
104	A’’		351	404	416	350	348	γCH(47)
105	A’’		300	398	402	297	296	γCH(51)
106	A’’		297	363	367	292	291	γCO(60), δOH(14)
107	A’’			287	284	270	269	γCO(47), δOH(12)
108	A’’			264	268	262	261	γCN(41)
109	A’’		250	263	265	253	250	γCC(60)
110	A’’			242	236	240	238	τCH_3(52)
111	A’’			237	232	230	228	$\gamma Ring3_{sym}$(54)
112	A’’			204	203	190	190	$\gamma Ring3_{sym}$(51)
113	A’’			190	197	181	180	$\gamma Ring3_{sym}$(47)
114	A’’		176	188	191	176	176	γCH(45)
115	A’’		149	171	177	150	147	γCN(60)
116	A’’			142	147	135	134	γCN(58)
117	A’’		122	127	129	122	120	γCH(47)
118	A’’			119	123	112	111	γCH(58)
119	A’’			109	116	103	101	γRing 1(56)
120	A’’		81	91	97	80	82	$\gamma Ring_{1}$(51)
121	A’’			83	87	70	69	γCC(49)
122	A’’			55	59	51	50	γCC(54)
123	A’’			21	23	23	22	γCC(38)

Molecular electrostatic potentials (MEPs)

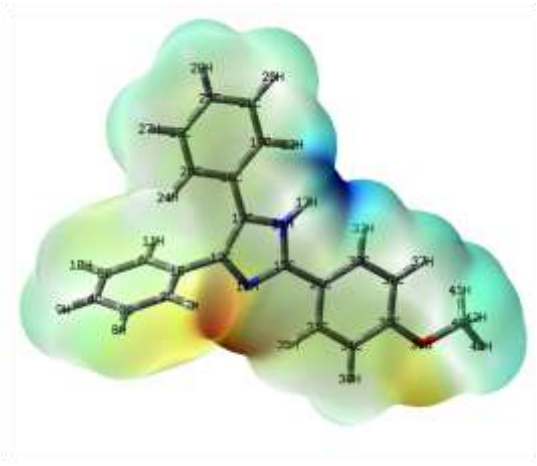

Fig. 5 DFT (B3LYP)/ccpVDZ calculated 3D molecular electrostatic potential of 2-(4-Methoxyphenyl)-4,5-diphenyl-1H-imidazole

Molecular electrostatic potential (ESP) at a point in the space around a molecule gives an indication of the net electrostatic effect produced at that point by the total charge distribution (electron + nuclei) of the molecule and correlates with dipole moments, electronegativity, partial charges and chemical reactivity of the molecules. It provides a visual method to understand the relative polarity of the molecule. An electron density isosurface mapped with electrostatic potential surface depicts the size, shape, charge density and site of chemical reactivity of the molecules. The different values of the electrostatic potential represented by different colors; red represents the regions of the most negative electrostatic potential, blue represents the regions of the most positive electrostatic potential and green represents the region of zero potential. Potential increases in the order red < orange < yellow < green < blue. Such mapped electrostatic potential surfaces have been plotted for title molecule in the B3LYP/6-311G basis set using the computer software Gauss view[10]. Projections of these surfaces along the molecular plane and a perpendicular plane are given in Fig. 5. This figure provides a visual representation of the chemically active sites and comparative reactivity of atoms. It may see that, in both methods, a region of zero potential envelopes the p-system of the aromatic rings, leaving a more electrophilic region in the plane of hydrogen atoms in MPDPI molecule. Direction of the dipole moment vector in a molecule depends on the centers of positive and negative charges. Dipole moments are strictly determined for neutral molecules. For charged systems, its value depends on the choice of origin and molecular orientation.

5. CONCLUSIONS

The present investigation thoroughly analyzed the vibrational spectra of MPDPI. All the vibrational bands observed in the FT-IR and FT-Raman spectra of the title compound are assigned to the various modes of vibration, and most of the modes have wavenumbers in the expected range. The complete vibrational assignments of wavenumbers are made on the basis of potential energy distribution (PED). The scaled B3LYP/ccpVDZ is the best over the other method. The molecular electrostatic potential surfaces helps us to identify the structural and symmetric properties of MPDPI.

REFERENCES

[1] Hochachka, P.W. & G.N. Somero 2002. *Biochemical adaptation: mechanisms and process in physiological evolution*. New York: Oxford University Press. 466 p.
[2] Castaño T, Encinas A, Pérez C, Castro A, Campillo NE, Gil C. Bioorg Med Chem. **16** (11) (2008) 6193-206.
[3] Bogle RG, Whitley GS, Soo SC, Johnstone AP, Vallance P. *Br J Pharmacol*. **111** (4) (1994) 1257-61.
[4] Khalid MH, Tokunaga Y, Caputy AJ, Walters E. J Neurosurg. **103** (1) (2005) 79-86.
[5] Leon Shargel. Comprehensive Pharmacy Review (6th ed.). p. 930.
[6] C. James, C. Ravikumar, V.S. Jayakumar, I. Hubert Joe, J. Raman Spectroscope. 40 (2009) 537–545.
[7] M. J. Frisch, G. W. Trucks, H. B. Schlegal, G. E. Scuseria, M. A. Robb, J. R. Cheesman, V.G. Zakrzewski, J. A. Montgomerg, Jr., R. E. Strtmann, J. C. Burant, S. Dapprich, J. M. Milliam, A. D. Daniels, K. N. Kudin, M.. C. Strain, O. Farkas, J. Tomasi, V. Barone, M. Cossi, R. Camme, B. Mennucci, C. Pomelli, C. Adamo, S. Clifford, J. Ochterski, G.A. Petersson, P. Y. Ayala, Q. Cui, K. Morokuma, N. Rega, P. Salvador, J. J. Dannenberg, D. K. Malich, A. D. Rabuck, K. Raghavachari, J.B. Foresman, J. Cioslowski, J. V. Ortiz, A. G. Baboul, B. B. Stefanov, G. Liu, A. Liashenko, P. Piskorz, I. Komaromi, R. Gomperts, R. L. Martin, D. J. Fox, T. Keith, M. A. Al– Laham, C. Y. Peng, A. Nsnsyskkara, M. Challacombe, P. M. W. Gill, B. Johnson, W. Chen, M.W. Wong, J. L. Andres, C. Gonzalez, M. Head–Gordon, E. S. Replogle and J. A. Pople, (2009) GAUSSIAN 09, Revision A.02, Gaussian, Inc., Pittsburgh.
[8] T. Sundius, J. Mol. Struct. 218 (1990) 321. MOLVIB: A Program for Harmonic force field calculations. QCPE Program No. 604 (1991).
[9] T. Sundius, Vib. Spectrosc. 29 (2002) 89–95.
[10] A. Frisch, A.B. Neilson, A.J. Holder, GAUSSVIEW user Manual, Gaussian Inc., Pittsburgh, CT, 2009.
[11] M. Silverstein, G. Clayton Bassler, C. Morrill, Spectrometric Identification of Organic Compound, Wiley, New York, 1981.2560.
[12] J. Mohan, Organic Spectroscopy-Principles and Applications, second ed., Narosa Publishing House, New Delhi, 2001.
[13] B. Revathi, V. Balachandrna, B. Raja, K. Anitha, M. Kavimani, J. Mol. Struct. 1141 (2017) 81–92.
[14] N. Puviarasan, V. Arjunan, S. Mohan, Turk. J. Chem. 26 (2002) 323–334.
[15] G. Varsanyi, Vibrational Spectra of Benzene Derivatives, Academic Press, New York, 1969.
[16] A. Altun, K. Golcuk, M. Kumru, J. Mol. Struct. 637 (2003) 155–169.

[17] F.R. Dollish, W.G. Fateley, F.F. Bentley, Characteristic Raman Frequencies on Organic Compounds, John Wiley, New York, 1997.
[18] M. Silverstein, G. Clayton Bassler, T.C. Morril, Spectroscopic Identification of Organic Compounds, John Wiley, New York, 1991.
[19] A. Altun, K. Golcuk, M. Kumru, J. Mol. Struct. (Theochem.) 625 (2003) 17–20.
[20] J.R. Durig, M.M. Bergana, H.V. Phan, J. Raman Spectrosc. 22 (1991) 141–146.
[21] G. Varsanyi, Vibrational Spectra of Benzene Derivatives, Academic Press, New York, 1969.
[22] A. Lakshmi, V. Balachandran, A. Janaki, J. Mol. Struct. 1004 (2011) 51–66.
[23] B. Revathi, V. Balachandran, B. Raja, K. Anitha, Ind. J. Pure Appl. Phys. 55 (2017) 49–53.
[24] D.N. Sathyanarayana, Vibrational Spectroscopy Theory and Applications, 2nd ed., New Age International (P) Limited Publisher, New Delhi, 2004.
[25] R.L. Peesole, L.D. Shield, I.C. McWilliam, Modern Methods of Chemical Analysis, Wiley, New York, 1976.
[26] G. Socrates, IR and Raman Characteristics Group Frequencies Tables and Charts, 3rd ed., Wiley, Chichester, 2001. pp. 107–111.